SLAC–PUB–6328
December 1993
(E/T)

THE FORM FACTORS OF THE NUCLEONS*

GERASSIMOS G. PETRATOS

Stanford Linear Accelerator Center
Stanford University, Stanford, California 94309

ABSTRACT

Recent measurements of the electric $G_E(Q^2)$ and magnetic $G_M(Q^2)$ form factors of the nucleons are reviewed and compared to theoretical calculations based on non-perturbative QCD sum rules, diquark, relativistic constituent quark, and vector meson dominance (VMD) models. A short summary of ongoing and future measurements is also presented.

1. INTRODUCTION

The study of the electromagnetic form factors of the nucleons are of fundamental importance in understanding nucleon structure. The form factors contain all the information about the deviation from pointlike structure of the charge and magnetization current distributions of the nucleons. The hope is that measurements at sufficiently large momentum transfers can provide a microscopic understanding of the nucleon wave functions in terms of their constituent quark amplitudes.

The form factors are measured in elastic electron-nucleon scattering, which is mediated by the exchange of a virtual photon. The differential cross section is given in terms of the electric $G_E(Q^2)$ and the magnetic $G_M(Q^2)$ nucleon form factors

$$\frac{d\sigma}{d\Omega} = \sigma_{Mott}\frac{E'}{E}\Big[\frac{G_E^2+\tau G_M^2}{1+\tau} + 2\tau G_M^2 \tan^2\Big(\frac{\theta}{2}\Big)\Big] ,$$

where σ_{Mott} is the Mott cross section for a structureless nucleon given by

$$\sigma_{Mott} = \frac{\alpha^2\cos^2(\frac{\theta}{2})}{4E^2\sin^4(\frac{\theta}{2})} ,$$

where E is the incident electron energy, and E' and θ are the scattered electron energy and angle. The four momentum carried by the virtual photon is $Q^2 = \vec{q}^2 - \nu^2 = 4EE'\sin^2(\frac{\theta}{2})$, where $\vec{q}$ and ν are the momentum and energy transfers to the nucleon. The parameter τ is given in terms of the nucleon mass M: $\tau = Q^2/4M^2$.

* Work supported by Department of Energy contract DE–AC03–76SF00515.

Invited talk presented at the International Workshop on Electron-Nucleus Scattering Isola, d'Elba, Italy, July 5–10, 1993.

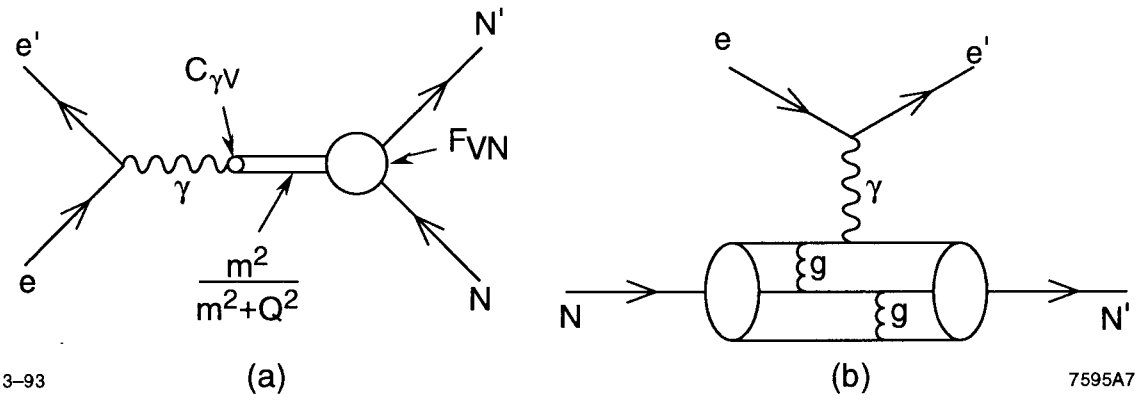

1) Elastic electron-nucleon scattering: (a) in the VMD scheme, where the virtual photon that mediates the interaction couples to the nucleon through vector mesons; (b) in the hard scattering scheme of quantum chromodynamics.

Early measurements of the proton form factors at small momentum transfers were found to be approximated by a dipole fit:

$$G_D(Q^2) = \left(1+\frac{Q^2}{0.71}\right)^{-2} \approx \frac{G_{Mp}(Q^2)}{\mu_p} \approx G_{Ep}(Q^2) ,$$

where μ_p=2.79 nm is the proton magnetic moment. The scaling relationship between the two form factors suggested that the charge and magnetization distributions have the same spatial dependence.

The neutron magnetic form factor was also found to be described fairly well by the dipole fit

$$\frac{G_{Mn}(Q^2)}{\mu_n} \approx G_D(Q^2) ,$$

indicating that the magnetic moment distribution of the neutron is similar to that of the proton. Here $\mu_n = -1.91$ nm is the magnetic moment of the neutron. The neutron electric form factor $G_{En}(Q^2)$ was found to be consistent with zero, in accordance with a zero net-charge distribution.

The virtual photon interaction is thought to be composed of two parts: one mediated by the exchange of vector mesons at low Q^2, and a part involving direct interaction with the nucleon or its constituents at large Q^2. In the VMD picture[1,2], the form factors are expressed in terms of photon-meson coupling strengths $C_{\gamma V}$ and meson-nucleon vertex form factors F_{VN} (see Fig. 1 (a)).

At large momentum transfers, dimensional scaling[3,4] predicts that the underlying mechanism in elastic electron-nucleon scattering is the hard re-scattering of the constituent quarks and that the nucleon form factors should fall with powers of Q^2 (*e.g.*, $G_M \sim 1/Q^4$). Within this hard scattering scheme (see Fig. 1 (b)), perturbative QCD describes the form factors as convolutions of the valence quark distribution amplitudes.[5]

Recent calculations have tried to describe the form factors in the intermediate Q^2 range. Gari and Krümpelmann (GK) have developed a phenomenological model[6] using the VMD form at low Q^2 and the asymptotic QCD form at high Q^2 to fit the existing data. Other approaches include the relativistic constituent quark model,[7,8] the use of QCD sum rules[9] to make absolute predictions, and a diquark model.[10]

2. RECENT MEASUREMENTS*

2.1 Rosenbluth Separations

Most of the existing data on the nucleon form factors have come from Rosenbluth separations in elastic electron-proton and quasielastic electron-deuteron scattering. A typical example based on this method is a recent SLAC experiment[13,14] that doubled the Q^2 range and improved the precision of previous measurements.

The experiment was performed at the Stanford Linear Accelerator and used beams from the nuclear physics injector with energies from 1 to 10 GeV and average currents from 1 to 10 μA. Electrons were scattered off 15-cm long liquid hydrogen and deuterium targets and were detected in the SLAC 1.6- and 8-GeV/c magnetic spectrometers.

The 8-GeV/c spectrometer was set at scattering angles between 15° and 90° and momenta between 0.5 and 7.5 GeV/c. The 1.6-GeV/c spectrometer, modified by adding a quadrupole doublet to quadruple its solid angle, detected electrons with momenta between 0.5 and 0.8 GeV/c and was fixed at 90°. Shower counters, Čerenkov counters, and wire chambers were used in both spectrometers to measure particle trajectories and to distinguish electrons from pions and other backgrounds.

2.1.1 Proton form factors

The proton form factors were determined by first converting the experimental elastic electron-proton cross sections, $\sigma(E,\theta)$, corrected for radiative effects, to reduced cross sections σ_R

$$\begin{aligned}\sigma_R(Q^2,\epsilon) &= \epsilon\left(1+\frac{1}{\tau}\right)\frac{E}{E'}\frac{\sigma(E,\theta)}{\sigma_{\rm Mott}} \\ &= G_{Mp}^2(Q^2)+\frac{\epsilon}{\tau}G_{Ep}^2(Q^2)\ ,\end{aligned}$$

where $\epsilon = \left[1+2(1+\tau)\ \tan^2\ (\theta/2)\right]^{-1}$ is the degree of longitudinal polarization of the virtual photon. Linear fits to the reduced cross sections at each value of Q^2 were

* Recent experiments and data from elastic measurements with detection of recoil nucleons in coincidence are presented in other contributions.[11,12]

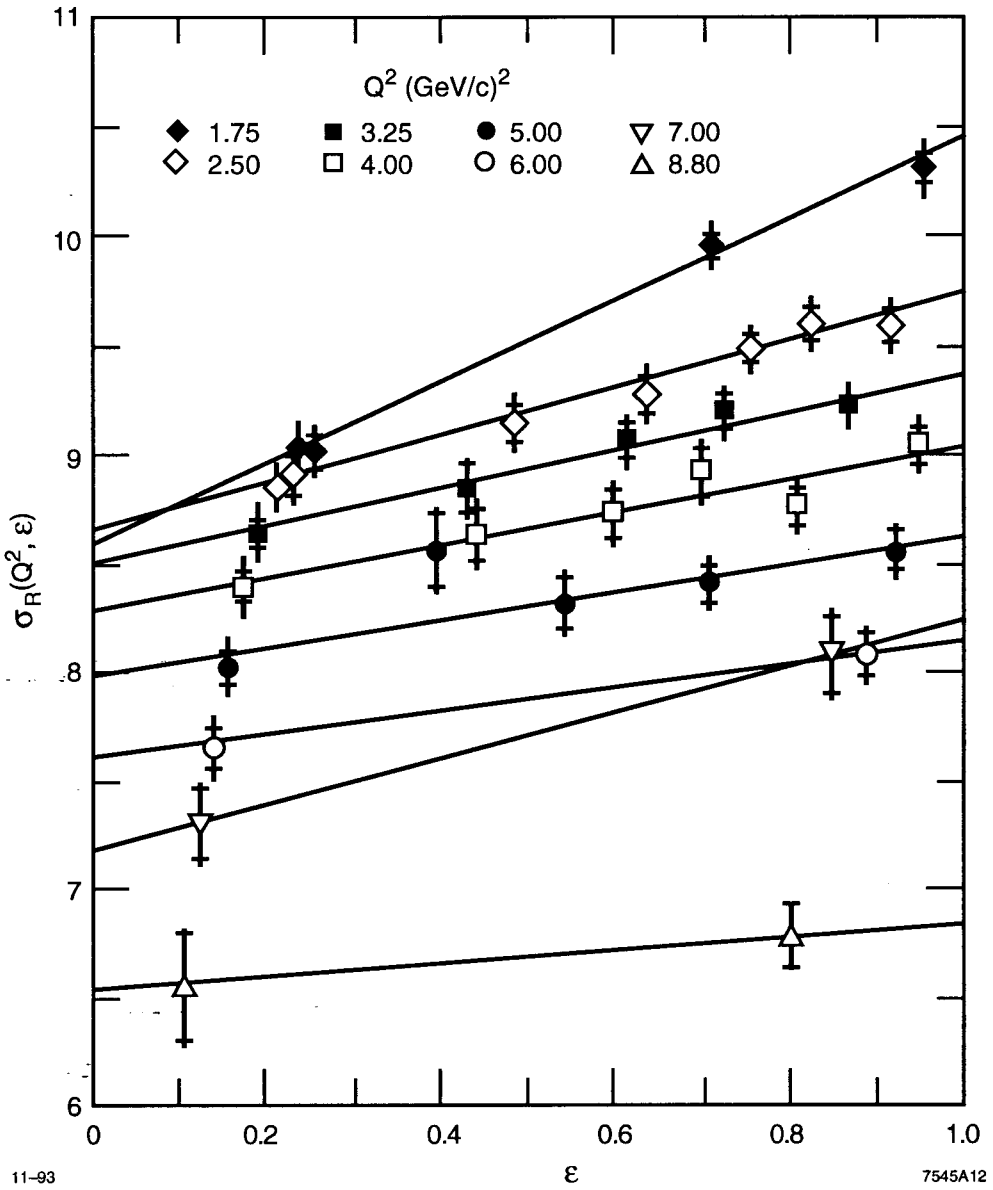

2) SLAC data and linear fits of reduced elastic electron-proton cross sections. At each Q^2, the intercept and slope yield the squares of the magnetic and electric proton form factor respectively.

performed (see Fig. 2) to obtain G_{Ep} from the slope and G_{Mp} from the intercept (Rosenbluth separation method). The extracted[13] proton form factors, scaled by the dipole fit, are shown in Figs. 3 and 4. The results at $Q^2 = 8.8$ (GeV/c)^2 were obtained by combining the backward angle data with previous forward angle cross section data[15] cross-normalized at the same Q^2= 5 (GeV/c)^2 value.

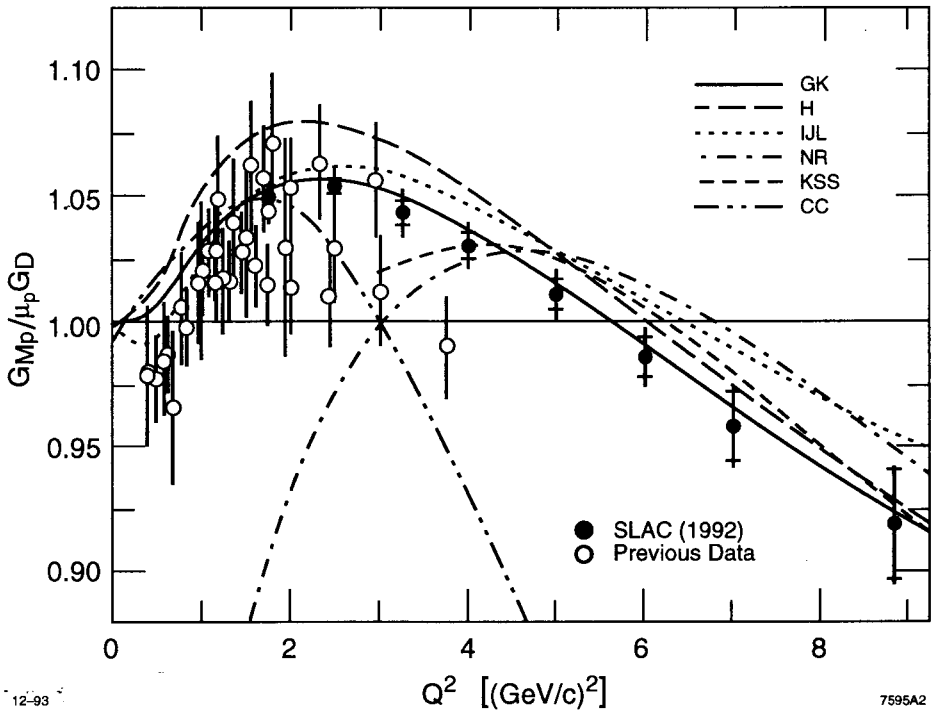

3) Proton magnetic form factor SLAC data, scaled by the dipole fit, along with previous data and theoretical calculations (see text). Inner error bars correspond to statistical uncertainties. Outer error bars include point-to-point systematic uncertainties.

The new data for G_{Mp} are in fairly good agreement with three commonly used VMD fits to previous data: Höhler *et al.*[2] (H, long dashed curves), Iachello, Jackson, and Lande[1] (IJL, dotted curves), and the GK fit[6] (GK, solid curves). The data for G_{Ep} lie above all these fits for $Q^2 > 3$ (GeV/c)^2, and are in especially poor agreement with the IJL fit. The simple dipole form actually shows the best agreement with the G_{Ep} data.

For $Q^2 \geq 4$ (GeV/c)^2, both G_{Mp} and G_{Ep} are in fair agreement with the prediction of Nesterenko and Radyushkin,[9] (NR, dash-dotted curves), which attempted to calculate the contribution to the nucleon form factors from soft non-perturbative processes. They used QCD sum rules based on quark-hadron duality to fix the parameters of the soft quark wave functions in calculating the form factors.

One of the diquark model fits of Kroll *et al.*[10] (KSS, short dashed curves) is in better agreement with the G_{Mp} data than the G_{Ep} data. This model views the proton as built up from quarks and diquarks. The diquarks are treated as quasi-elementary constituents. Their composite nature is taken into account by diquark form factors. The diquarks are viewed as an effective description of correlations in the nucleon wave function and constitute a model for non-perturbative effects.

Relativistic constituent-quark calculations are sensitive to parameters such as the effective quark masses m_i, quark wavefunction, and confinement scale a. For example, the model by Chung and Coester[6] assumes a simple exponential wave function of the form $\phi(M_o) = N \exp(-M_o^2/2a^2)$, where $M_o^2 = \sum_i \sqrt{m_i^2 + \vec{q}_i^2}$ with $\vec{q}_i$ being the quark relative momenta. The model using a representative choice of parameters (CC, dash double-dotted curves) lies above the G_{Ep} data, and underestimates G_{Mp} above $Q^2 = 2$ (GeV/c)^2.

2.1.2 Neutron form factors

Quasi-elastic electron-deuteron cross sections, sensitive to the incoherent sum of scattering from a proton and a neutron, were extracted[14] from the radiatively corrected measured inclusive spectra, after subtracting the inelastic contributions. These contributions were calculated using a Fermi smearing model to convolute measured proton resonance region data with the deuteron wavefunction $\psi(k)$, and were fitted to the deuterium data in the same region.

A reduced cross section per nucleon for quasielastic scattering was defined as:

$$\begin{aligned} \sigma_R(Q^2, \nu, \epsilon) &= \epsilon(1+\tau') \frac{\sigma(E, E', \theta)}{\sigma_{\text{Mott}}} \\ &= R_T + \epsilon R_L \ , \end{aligned}$$

where $\tau' = \nu^2/Q^2$. The neutron form factors were extracted[14] by a Rosenbluth separation of the nuclear response functions R_T, R_L using the proton form factor measurements from the same experiment and a simplified form of McGee's nonrelativistic plane wave impulse approximation quasielastic model[16]

$$R_T = \frac{M^2\tau'}{2q} (G_{Mp}^2 + G_{Mn}^2) \int_{k_{\min}}^{k_{\max}} \frac{u^2(k) + w^2(k)}{\sqrt{k^2 + M^2}} \, k \, dk \ ,$$

and

$$R_L = \frac{M^2}{2q} (G_{Ep}^2 + G_{En}^2) \int_{k_{\min}}^{k_{\max}} \frac{u^2(k) + w^2(k)}{\sqrt{k^2 + M^2}} \, k \, dk \ ,$$

where u and w are the S and D state of the deuteron wavefunction and $k_{\min}, k_{\max}$ are the extreme values of the Fermi momentum of the struck nucleon. The results were fairly insensitive to the choice of different $\psi(k)$'s used in the quasielastic model (Paris, Bonn and Reid soft core nucleon-nucleon potentials). A greater sensitivity was observed in the shape of the inelastic model, although the sensitivity resulted in uncertainties smaller than the experimental ones.

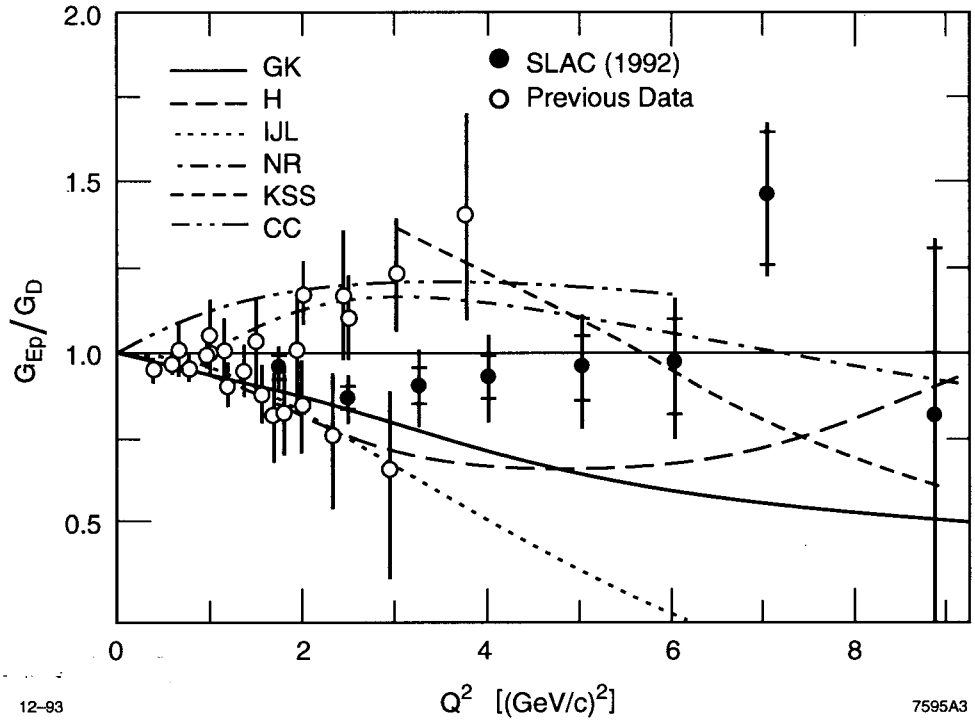

4) Proton electric form factor SLAC data, scaled by the dipole fit, along with previous data and theoretical calculations (see text). Inner error bars correspond to statistical uncertainties. Outer error bars include point-to-point systematic uncertainties.

The two nuclear response functions, including inelastic contributions, are shown in Fig. 5 as a function of missing mass squared $W^2 = M^2 + 2M\nu - Q^2$. The solid curves are model calculations of the combined quasielastic and inelastic contributions for $G_{En} = 0$ and $G_{Mn} = (\mu_n/\mu_p)G_{Mp}$. It is evident that this form factor choice describes the data well. The dotted curves were calculated using the same models as the solid curves, except that the GK parametrizations of G_{En} and G_{Mn} were used. It is clear that this parametrization, which predicts large values for G_{En}, is ruled out.

The neutron form factor data, shown in Figs. 6 and 7, exhibit much larger discrepancies with models than do the proton form factor data. Among the VMD models, the IJL model (dotted curves) is very poor at high Q^2 for G_{Mn}, while the Höhler fit (H, dashed curves) is considerably better for both form factors. The GK fit (solid curves) is completely ruled out by the G_{En} data.

The diquark model (KSS, short-dash curves) that did reasonably well for the proton does extremely poorly for both G_{En} and G_{Mn}. Like the GK fit, the relativistic constituent quark model (CC, dash-double dotted curves) predicts

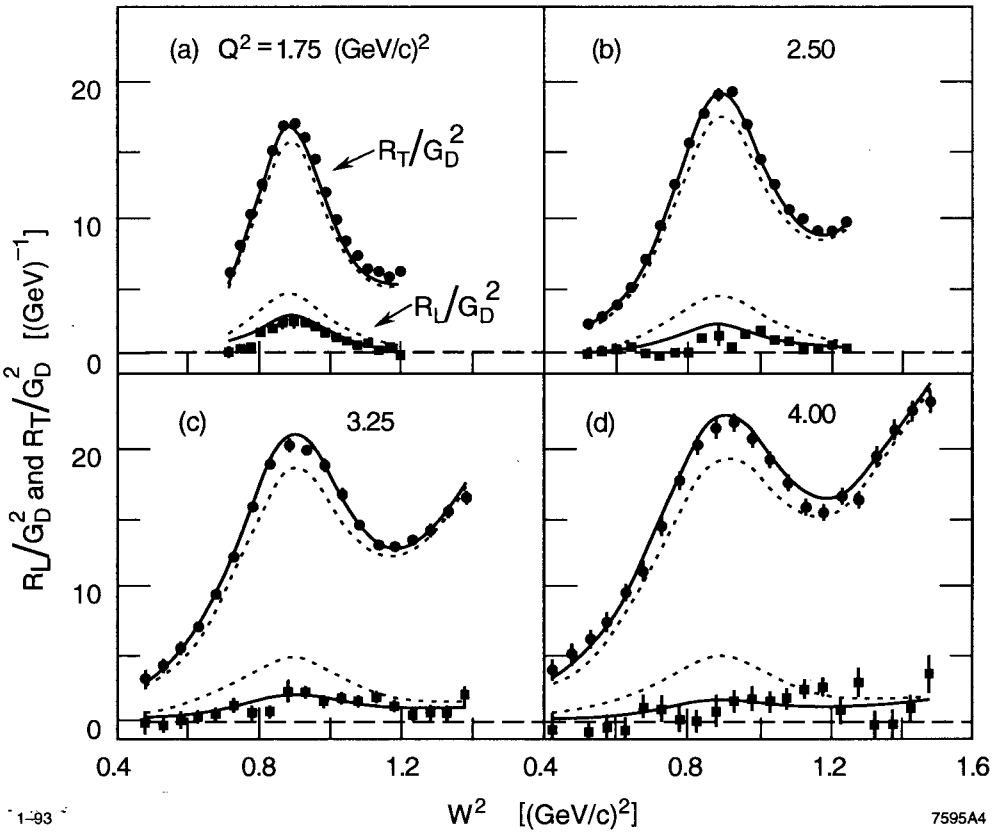

5) The nuclear response functions R_L and R_T for inclusive electron-deuteron scattering. The Q^2 values are at the top of the quasielastic peak and vary slightly with W^2. The curves are described in the text.

$G_{En} = -\tau G_{Mn}$, and is also in poor agreement with the data for G_{En}. Finally, the non-perturbative QCD Sum Rule predictions (NR, dash-dotted curves) are in agreement with G_{En}, and approach the G_{Mn} data at higher Q^2, where the calculations are expected to be valid.

The best description of the data, however, is simply given by the dipole fit for G_{Mn} and $G_{En}^2 = 0$. A careful comparison of Figs. 3, 4 and 6 shows that the present data for G_{Mn}, G_{Ep}, and G_{Mp} are all consistent with form factor scaling, perhaps implying that the spatial charge and magnetization distribution of the proton are similar even at small distance scales.

2.2 G_{En} From Elastic Electron-Deuteron Scattering

One way to extract G_{En} at small momentum transfers is from forward angle elastic electron scattering from deuterium. To the extent that the scattering is described by the impulse approximation, the deuteron electric form factor $A(Q^2)$ is given in terms of the elastic form factors of the nucleon and the deuteron wave function

$$A \sim (G_{Ep} + G_{En})^2 f[(\psi(k))] \; .$$

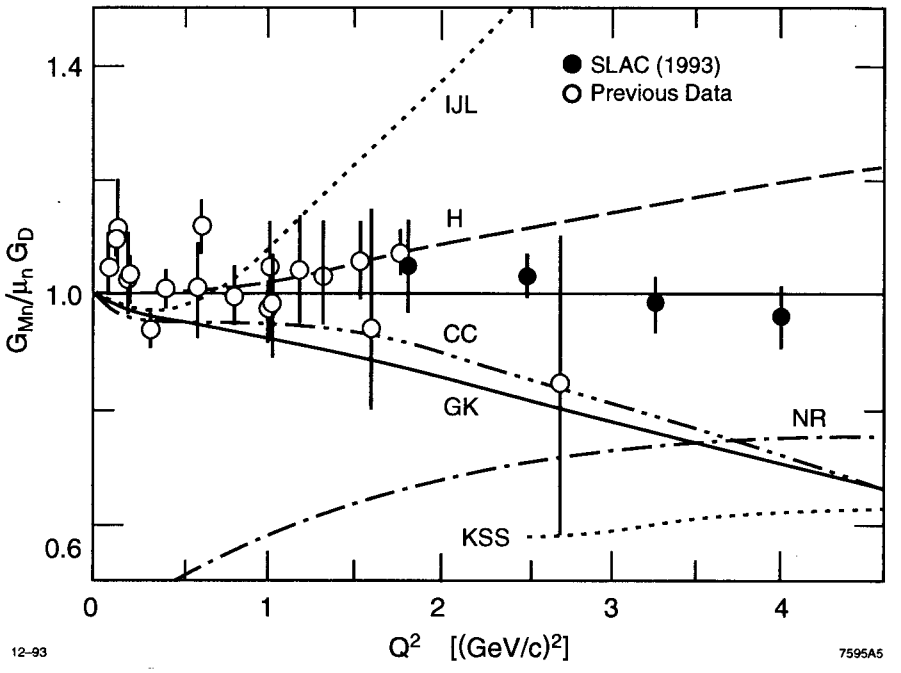

6) Neutron magnetic form factor SLAC data, scaled by the dipole fit, along with previous data and theoretical calculations (see text). Inner error bars correspond to statistical uncertainties. Outer error bars include point-to-point systematic uncertainties.

Calculations have shown that corrections from meson-exchange currents and relativistic effects are small (of the order of ~10%) in the range $0 < Q^2 < 1$ (GeV/c)^2, and that G_{En} can be calculated given a nucleon-nucleon potential.

Such an experiment was performed at Saclay.[17] Data fits are shown in Fig. 8 for several deuteron wavefunctions. Despite the strong sensitivity in the nucleon-nucleon potential choice, the data have provided the first conclusive evidence for non-zero G_{En} values for finite Q^2.

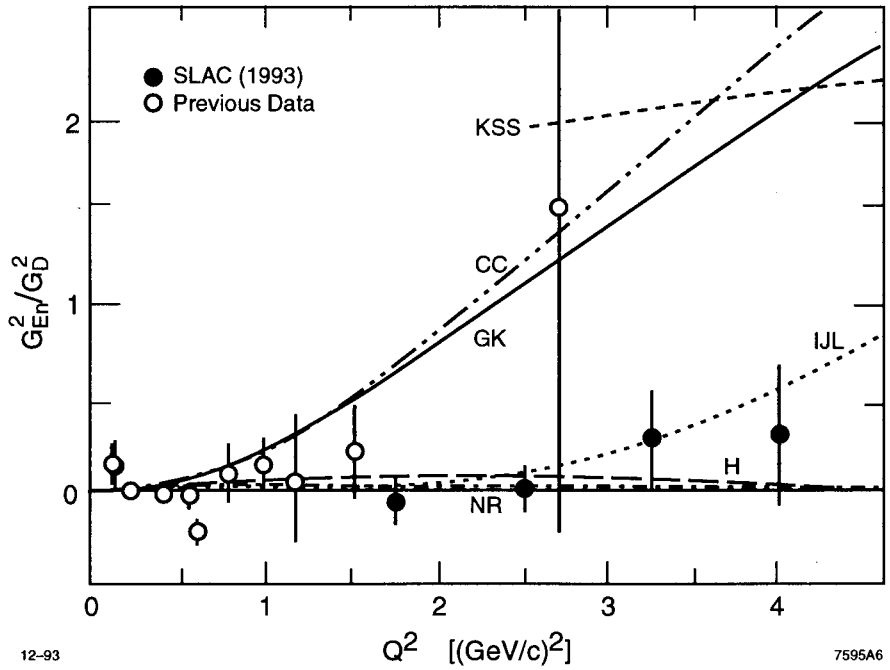

7) Neutron electric form factor SLAC data, scaled by the dipole fit, along with previous data and theoretical calculations (see text). Inner error bars correspond to statistical uncertainties. Outer error bars include point-to-point systematic uncertainties.

3. FUTURE MEASUREMENTS

3.1 G_{Mn} From Backward Inclusive Electron–Deuteron Scattering

The high beam intensity of CEBAF ($\sim 200\mu$A) and the availability of a high-power cryogenic deuterium target can be used to push the extraction of G_{Mn} from inclusive quasielastic scattering to its practical limit of about $Q^2 = 6.5$ (GeV/c)^2. To minimize the unknown contribution to the cross section from G_{En}, the measurements[18] will use the large solid angle, Hall A electron spectrometer at a backward angle of $\sim 120°$, eliminating the need of a Rosenbluth separation.

3.2 Experiments With Polarized Targets

Recent advances in polarized deuterium or ^{3}He targets allow for measurements of the neutron form factors by measuring the cross section asymmetry in quasielastic scattering of longitudinally polarized electrons off polarized neutrons in such targets.

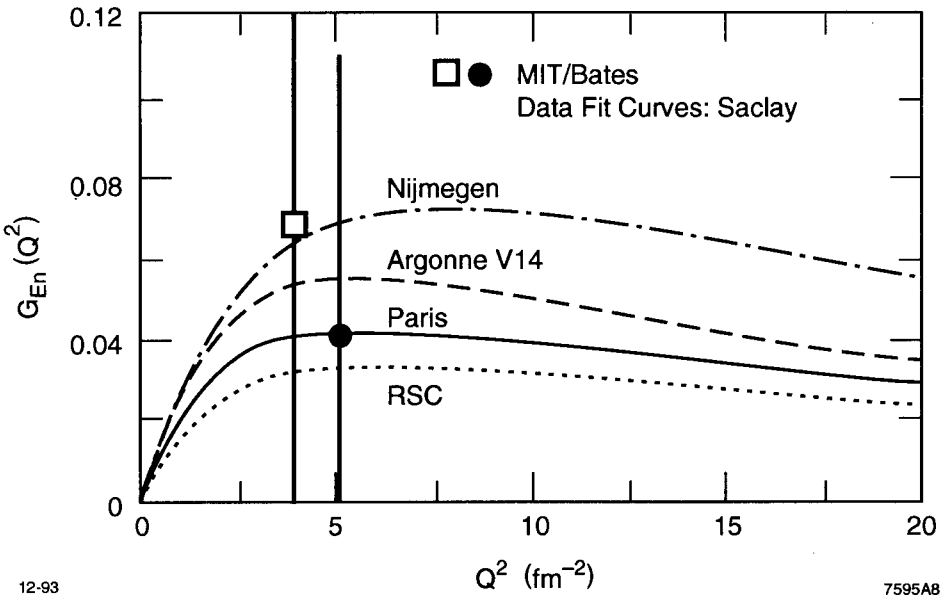

8) Low Q^2 neutron electric form factor data. The curves are fits of data extracted from elastic electron-deuteron scattering for four nucleon-nucleon potential models. The data points are from two recent experiments at MIT/Bates with a polarized beam and a polarized ^{3}He target.

For example, the asymmetry A_σ when the target is polarized perpendicular to $\vec{q}$ is given by:

$$A_\sigma = \frac{-2\sqrt{\tau(1+\tau)}\tan(\frac{\theta}{2})G_{En}G_{Mn}}{G_{En}^2 + \tau\left[1+2(1+\tau)\tan^2(\frac{\theta}{2})\right]G_{Mn}^2}\ .$$

Similar relations hold for other target spin orientations allowing for an independent determination of both nucleon form factors with this technique.

Experiments at MIT/Bates,[19,20] performed with two different polarized ^{3}He targets, though limited by statistics (see Fig. 8), have already demonstrated the feasibility of the technique. New measurements from ongoing experiments at Bates[21] and Mainz[12] are expected to provide precise data for G_{En} in the Q^2 range up to $\sim$ 0.5 (GeV/c)^2. With the advent of CEBAF, this technique can be pushed[22] to higher momentum transfers ($Q^2 \gtrsim 2$ (GeV/c)^2).

Large deuterium polarization ($\sim$ 30%) exhibited in a recently constructed polarized deuterated ammonia (ND_3) target are expected to provide precise data[23] on G_{En} for momentum transfers as large as $Q^2 \gtrsim 2$ (GeV/c)^2 at CEBAF. The target is being successfully used to measure the spin structure functions of the neutron at SLAC.

3.3 Experiments With A Recoil Polarimeter

More than ten years ago, Arnold, Carlson and Gross[24] suggested the polarization transfer technique to measure the nucleon form factors. This method requires a longitudinally polarized electron beam scattered off an unpolarized nucleon target, and a polarimeter to measure the polarization transferred to the recoiling nucleon.

The two components of the nucleon polarization in the scattering plane, the transverse P_x and the longitudinal P_z, were shown to be functions of the nucleon form factors

$$P_x = -\frac{2}{I_o}\sqrt{\tau(1+\tau)}G_M G_E \tan\left(\frac{\theta}{2}\right)$$
$$P_z = \frac{E+E'}{MI_o}\sqrt{\tau(1+\tau)}G_M^2 \tan^2\left(\frac{\theta}{2}\right) \quad ,$$

where $I_o = G_E^2 + \tau G_M^2/\epsilon$. The advantage of this method is that a measurement of P_x yields G_E directly, unlike cross section measurements which yield G_E^2.

The P_x polarization is measured from the azimuthal angular distribution of the nucleons scattered off the polarimeter

$$N(\Theta,\Phi) = N(P_e = 0,\Theta)\left[1 + P_e P_x A_p \sin\Phi\right] \ ,$$

where P_e is the incident beam polarization and A is the analyzing power of the polarimeter.

The first experiments measuring recoil polarization in quasielastic scattering from deuterium are being done at Bates[25] and Mainz[12] to obtain the neutron electric form factor. An extension at higher momentum transfers up to $Q^2 = 2$ (GeV/c)^2 is planned[26] at-CEBAF. Similar measurements on the electric form factor of the proton are expected at Bates[27] (low Q^2), and at CEBAF[28] up to $Q^2 = 6$ (GeV/c)^2.

4. CONCLUSIONS

Recents measurements from Rosenbluth separations in elastic electron-proton and quasielastic electron-deuteron scattering have doubled the Q^2 range of previous data and considerably reduced the error bars in the region of overlap. The results for $G_{Mp}/\mu_p G_D$ decrease smoothly with increasing Q^2, while G_{Ep} and G_{Mn}/μ_n are consistent both with the dipole form G_D and with form factor scaling.

The results for G_{En}^2/G_D^2 exclude models that predict large values like the popular parametrization by Gari and Krümpelmann. Low Q^2 data from elastic electron-deuteron scattering have shown non-zero values for G_{En}. None of the existing models is in good agreement with all form factor results at all values of Q^2, although for sēvēral of the models, this could be remedied by adjusting free parameters.

Ongoing and future experiments at several laboratories are expected to extend G_{Mn} measurements at higher momentum transfers and to reduce the experimental errors on the electric nucleon form factors. The latter is feasible by using polarized beams and recent advances in polarized targets or recoil nucleon polarimeters. New improved nucleon form factor data will provide better constraints on models of the nucleon structure and better inputs in calculations of the wave functions of light nuclei (deuterium and helium).

5. REFERENCES

1. F. Iachello, A. Jackson and A. Lande, Phys. Lett. **43B**, 191 (1973).
2. G. Höhler *et al.*, Nucl.Phys. **B114**, 505 (1976).
3. S. J. Brodsky and G. Farrar, Phys. Rev. Lett. **31**, 1153 (1973); Phys. Rev. **D11**, 1309 (1975).
4. V. A. Matveev, R. M. Muradyan and A. N. Tavkhelidze, Lett. Nuovo Cimento **7**, 719 (1973).
5. G. P. Lepage and S. J. Brodsky, Phys. Rev. **D22**, 2157 (1980).
6. M. Gari and W. Krümpelmann, Z. Phys. **A322**, 689 (1985); Phys. Lett. **B173**, 10 (1986).
7. P. L. Chung and F. Coester, Phys. Rev. **D44**, 229 (1991).
8. F. Schlumpf, SLAC–PUB–6335 (1993).
9. V. A. Nesterenko and A. V. Radyushkin, Phys. Lett **128B**, 439 (1983); Sov. J. Nucl. Phys. **39**, 811 (1984).
10. P. Kroll, M. Schürmann and W. Schweiger, Z. Phys. **338**, 339 (1991).
11. J. Jourdan, presentation to this Workshop.
12. T. Walcher, presentation to this Workshop.
13. P. E. Bosted *et al.*, Phys. Rev. Lett. **68**, 3841 (1992).
14. A. F. Lung *et al.*, Phys. Rev. Lett. **70**, 718 (1993).
15. A. F. Sill *et al.*, Phys. Rev. **D48**, 29 (1993).
16. I. McGee, Phys. Rev. **161**, 1640 (1967); A. F. Lung, SLAC–NPAS–TN–91–2 (1991).
17. S. Platchkov *et al.*, Nucl. Phys. **A510**, 740 (1990).
18. J. Gomez, G. Petratos *et al.*, The Hall A Collaboration, CEBAF Experiment 93-24.
19. C. E. Jones *et al.*, Phys. Rev. **C44**, 571 (1991).
20. A. K. Thompson *et al.*, Phys. Rev. Lett. **68**, 2901 (1992).

21. C. E. Jones, presentation to this Workshop.

22. R. D. McKeown *et al.*, CEBAF Experiment 91–20.

23. D. B. Day *et al.*, CEBAF Experiment 93–26.

24. R. G. Arnold, C. E. Carlson and F. Gross, Phys. Rev. **C21**, 1426 (1980).

25. R. Madey *et al.*, MIT/Bates Experiment 89–04.

26. R. Madey *et al.*, CEBAF Experiment 93–38.

27. J. M. Finn *et al.*, MIT/Bates Experiment 88–21.

28. C. Perdrisat, V. Punjabi *et al.*, The Hall A Collaboration, CEBAF Experiment 93–27.